U.S. GEOLOGICAL SURVEY

SAUDI ARABIAN PROJECT REPORT 274

EVALUATION OF THE WADI MANDAHAH ANCIENT MINE, KINGDOM OF SAUDI ARABIA

by

Mustafa M. Mawad

with a section on a

GEOPHYSICAL SURVEY

by

Habib M. Merghelani

U.S. Geological Survey Open-file Report 80-1262

This report is preliminary and has not been reviewed for conformity with U.S. Geological Survey editorial style. Use of trade names is for descriptive purposes only and does not constitute endorsement by the USGS.

U.S. Geological Survey
Jidda, Saudi Arabia

1980

The work on which this report is based was performed in accordance with a cooperative agreement between the U. S. Geological Survey and the Ministry of Petroleum and Mineral Resources, Kingdom of Saudi Arabia.

CONTENTS

ILLUSTRATIONS

TABLES

EVALUATION OF THE WADI MANDAHAH ANCIENT MINE,

KINGDOM OF SAUDI ARABIA

by

Mustafa M. Mawad

ABSTRACT

The Wadi Mandahah mine is an ancient gold mine that probably was worked during the Abbasid Caliphate in the eighth and ninth centuries A.D.

The mine is in complexly folded and faulted metavolcanic and pyroclastic rocks of the Baish group of Precambrian age. The mineralized outcrop consists of weakly limonitic gossan containing malachite and chrysocolla veinlets. The deposit has been mined in shallow pits and trenches. Geochemical and geophysical surveys indicated weak mineralization along shear zones and in the nose of a fold that plunges southwest. Four holes aggregating 887.4 m were drilled to explore the mineralized zones below ancient workings. No significant ore bodies were discovered.

INTRODUCTION

Location and description

Wadi Mandahah ancient mine is located at lat 20°19'10" N. and long 41°45'00" E. in Bilad Zahran, 200 km southeast of Taif along the Hijaz paved highway and about 40 km northwest of Al Bahah (fig. 1). Several unpaved roads constructed by the Ministry of Agriculture and by farmers permit access to the area by 4-wheel drive vehicles.

The mining site is 2 km north of Al Hassan village and 2.5 km east of Mahawiah village. The main and largest village in the district, Al Atawlah (or Suq al Rabooa, "Wednesday market"), is 10 km to the south.

The area is inhabited by settlers from the Al Zahran tribe. Farming is their main occupation and almost all the wadis are cultivated. Terraces are constructed along the wadis to provide level ground for cultivation and to hold and spread water.

Water wells provide irrigation for grapes, peaches, pomegranates, apricots, alfalfa, figs, and vegetable crops near the wells. Millet and other similar grains are raised on cultivated land away from the wells during the rainy seasons. Farmers live in houses built of large slabs of schist stacked tightly without mortar. Ruins of the same

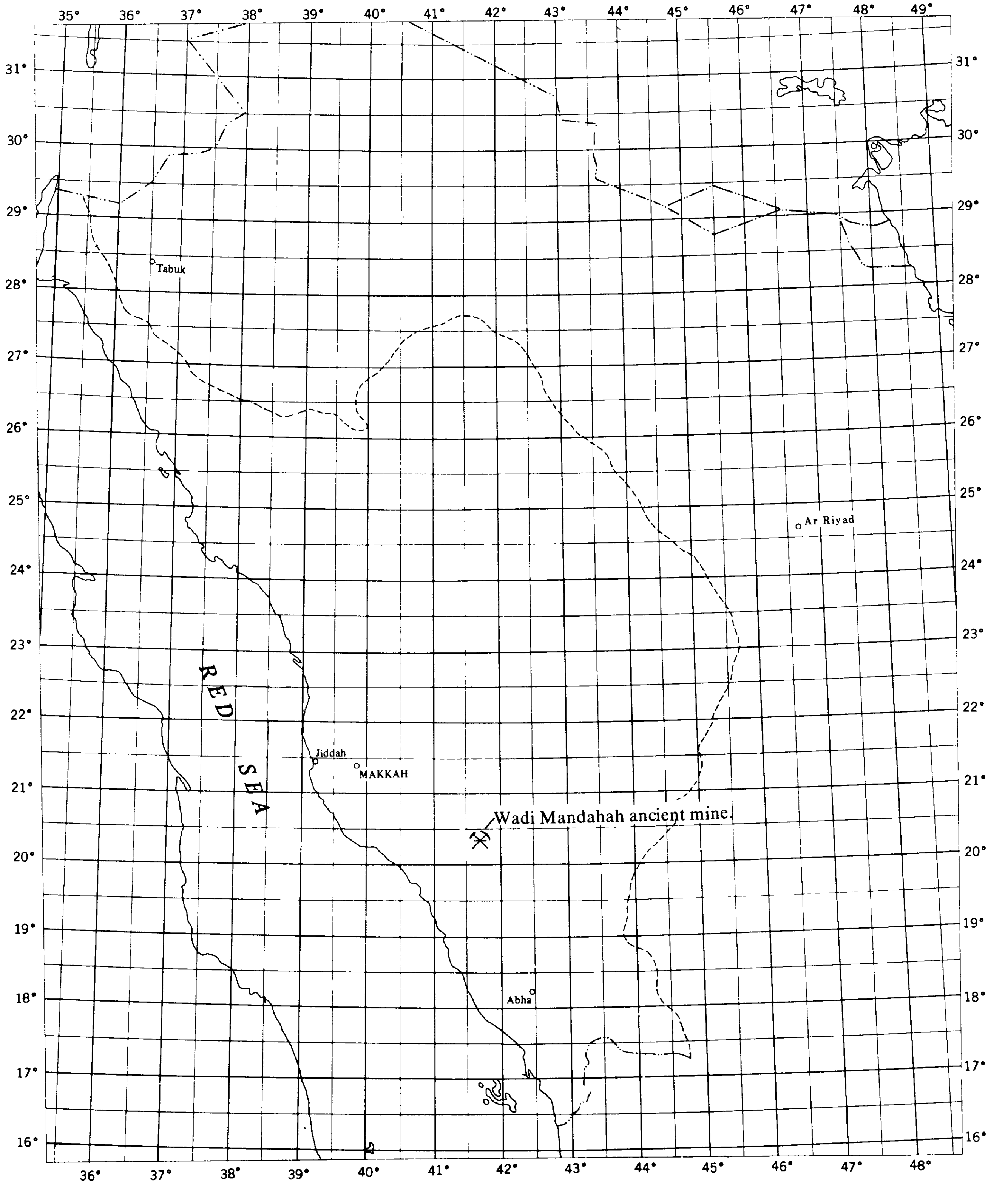

Figure 1.–Index map showing location of Wadi Mandahah ancient mine.

style occur around the mining site. Grinding stones are common and indicate that a considerable amount of milling took place. Small amounts of slag were found near the Wadi Mandahah mine and nearby small mines.

Previous investigation

The regional geology of the Wadi Mandahah district was first described by Brown and others (1963). Smith (1964) and Jackaman (1972) briefly described the area and other mines in the vicinity. Mawad (1975) presented a structural and mineralogical study in a thesis for a masters degree.

Purpose of study

The Wadi Mandahah mine was worked extensively, probably during the Abbasid Caliphate in the eighth or ninth century. The mineralized zone extends for more than 300 m along strike, and outcrops were sufficiently encouraging to indicate that additional studies were warranted. Therefore, the area was mapped geologically at a scale of 1:1000 on a grid base by means of tape and compass. In addition, geochemical and geophysical studies were undertaken. This paper summarizes the results of geologic mapping, geochemical and geophysical surveys, and diamond drilling.

Acknowledgements

This study was undertaken in accordance with an agreement between the Ministry of Petroleum and Mineral Resources and the U.S. Geological Survey (USGS). The writer is grateful for assistance provided by the analytical laboratory of the Directorate General of Mineral Resources and the mineralogical laboratory of the USGS Mission. The writer also greatly appreciates the assistance provided by T. H. Kiilsgaard and F. S. Simons, former Chiefs of the USGS Mission, R. G. Worl, project supervisor, and the staff of the Institute of Applied Geology, headed by A. Al Shanti.

GEOLOGY

Regional framework

The Wadi Mandahah district is underlain by Precambrian rocks of the Baish and Bahah groups and by several kinds of granitic rocks and dike rocks.

Rocks of the Baish group (Greenwood, 1975) include interlayered lava flows, volcanic breccia, and tuff. The lava flows are commonly massive and are of andesitic composition. In places they are amygdaloidal, and the amygdules are filled with radial growths of epidote and quartz. A few plagioclase phenocrysts about 0.5 cm long of albite-oligoclase composition were noted.

Volcanic breccia contains in some localities fragments ranging in diameter from less than a centimeter to more than 10 cm set in a fine-grained matrix of chloritized ash. The fragments are composed mainly of quartz and some plagioclase. The rock is highly foliated, and the fragments have been considerably stretched and arranged in distinct lines. Commonly they are more abundant in some layers than in others. The fragments are thought to have formed either from primary breccia fragments or from secondary veins rich in quartz and plagioclase. During deformation, the fragments and veins were stretched, boudinaged, and separated into sausage-like forms.

Fine-grained andesitic ash or tuff, generally chloritized, epidotized in some localities, sericitized, and well foliated, is intercalated with flow rock and breccias. During metamorphism the original sedimentary lamination and graded bedding were preserved.

In the eastern part of the area the rocks are intercalated with amphibole-rich bodies, most of which are more than 50 m long. These amphibole-rich bodies are coarse grained at the center but have a gradational contact with the chlorite schist. They may be metamorphosed gabbroic bodies that cooled slowly in place. To the west the rocks are mainly chlorite schist that is increasingly of metasedimentary aspect and that contains calcareous materials. The contact between the metavolcanic and the sedimentary units is gradational, and in many places sedimentary rocks are intercalated with metavolcanic rocks. Several volcanic episodes, characterized by an alternation of the common lithologies (lavas, volcanic breccia, and fine tuff), were recognized in the Mandahah area.

The second unit exposed extensively in the area is the metasedimentary Bahah group, a thick section mostly of quartz-chlorite-sericite schist derived from volcanic siltstones and mudstones. The rocks are highly sheared and deformed, and most of the primary sedimentary features are obliterated. Beds of phyllite contain some graphitic and limy graphitic beds. Subordinate rocks include calcareous siltstone, limestone, and hematite-quartz-jaspilite. The contact between the Baish and Bahah groups is conformable and gradational, and is well exposed along road cuts of the new Taif-Abha highway.

Pyroclastics and tuff are dark gray, commonly with quartz-epidote clots stretched and oriented in the northwest direction. These clots are embedded in a groundmass composed of chlorite, epidote, quartz, and varying amounts of plagioclase (albite-oligoclase). Locally, zones that extend for several kilometers are enriched with pink potassium feldspar. The feldspar, which gradually decreases in amount at the edges of these zones and fills the cracks and the cleavage planes of the schist, may represent late hydrothermal activities. Minor pyrite is associated with this feldspathic zone. Iron formation consists of magnetite, along with quartz, and hematite that forms a small lens within the pyroclastics in the northeastern part of the mine area.

The rocks of the Baish and Bahah groups are intruded by large bodies of granite, granophyre, and diorite to quartz diorite and by several mafic dikes and dikes of rhyolite and porphyritic andesite. Many of the dikes are several kilometers long and 5 to 10 m wide.

Two generations of quartz veins are recognized. They are concentrated in the eastern part of the map area (fig. 1) and at several other localities in the district. The first generation is pretectonic, sheared, and contorted, whereas the second generation is posttectonic, massive, and milky. Neither contains significant mineralization.

Regional structure

The Wadi Mandahah prospect is just west of the Wadi Bidah mineral belt (Greenwood and others, 1974a). This belt extends northerly along Wadi Bidah in metavolcanic rocks of the Baish group and in intrusive bodies of dioritic, quartz dioritic, and granitic to granophyric composition. Massive sulfide deposits of Wadi Bidah are composed of pyrite, chalcopyrite, and sphalerite (Earhart and Mawad, 1970; Greenwood and others, 1974b).

Rocks in the central part of the Wadi Mandahah area are highly deformed. The area was subjected to a period of strong north-south compressional forces that folded the rocks into a series of anticlines and synclines plunging steeply north or south. North-trending faults cut the folds. Amount or sense of displacement is not obvious along these faults except on one fault that has strike-slip displacement of approximately 350 m. These faults extend several kilometers north and south of the area, and the width of the fault zones ranges from 1 m to about 10 m. Fault planes dip 70° west, and rocks along them are highly brecciated, sheared, and altered.

Two other sets of faults in the district intersect at acute angles of about 45°. The bisector of the acute angle is oriented east-west. These two sets of faults developed at the same time and form a conjugate system. Most of the faults of the conjugate system show no lateral movement, but along a few that cut dikes, displacements are about 5 to 10 m. These faults probably developed as a result of east-west compression during regional metamorphism, which also created strong shearing and lineation.

Schistosity is well developed in the less competent rocks such as volcanic breccia and tuff. In general, schistosity strikes north to N.20° E.

Geology of Wadi Mandahah mine

The rocks of the Wadi Mandahah mine area (fig. 2) consist mainly of chlorite schist of the Baish group, which is locally sericitized and oxidized. This rock contains elongated blebs rich in epidote. East of the map area, a large unit rich in sericite, potassium feldspar, and quartz is exposed. These two major rock units are cut by quartz veins of two generations, and by mafic and rhyolitic dikes. A small outcrop of iron formation is exposed at the northwest corner of the mapped area, and gossan crops out in the central part.

Regional structural features are represented by only one set of conjugate faults, which strike northeast and have very small sinistral displacement.

Mineralization and alteration

Mineralization is indicated at the surface by limonite gossans that contain sparse to abundant malachite and chrysocolla, mainly as stringers filling fractures and shear planes. This zone of alteration and oxidation strikes northerly, dips 80° W., is about 300 m long, and has an average width of about 10 m. Anomalous amounts of copper and zinc occur only in parts of this gossan (see fig. 2).

Disseminated sulfides, mainly pyrite cubes, occur in all rock types. The amount of sulfide ranges mostly from 1 to 2 percent but may be as great as 20 percent or more. Sulfides are localized along shear planes and cleavage.

Drilling program

The drilling program at Wadi Mandahah ancient mine was carried out by the Arabian Drilling Company (ADC) between June and November 1974. Four holes, totaling 887.4 m and designed to test the possible extension of mineralization under the old workings, were drilled. Hole Mh 1 tested the main gossan and the strongest geophysical anomaly. Mh 2 and Mh 3 tested the extension of the mineralization north of the main gossan under the cultivated land and also tested several small mineralized shear zones. Mh 4 was located to test the same zone as tested by Mh 1 but at greater depth. The lithologic logs of these holes are summarized in tables 1, 2, 3, and 4.

Hole Mh 1 (fig. 3) was drilled from the east side of the gossan to intersect the mineralized zone at a depth of about 100 m below the surface. The hole deviated upward and at about 60 m from the surface a zone in which no core was recovered was intersected between drillhole depths of 191.85 m and 193.05 m. Gravel and charcoal fragments from this interval suggest that an ancient working was cut. The rocks on both sides of this interval are copper stained and highly oxidized.

Holes Mh 2 (fig. 4) and Mh 3 (fig. 5) were sited along the northern part of the gossan zone to determine whether the gossan extends under the cultivated area and to test the copper-stained zones west of the farm. These holes intersected only a little pyrite disseminated through all rock types.

Hole Mh 4 was drilled to confirm the data reported from hole Mh 1 and to intersect the mineralized zone at a lower level. Several mineralized and sheared zones were intersected, and are shown in figure 6. Mineralization is mainly pyrite, chalcopyrite, sphalerite, and galena.

GEOCHEMISTRY

Surface sampling

Two hundred samples were collected from outcrops at Wadi Mandahah ancient mine for geochemical analyses. Of these, 175 chip samples were collected at intervals along parallel lines 40 m apart and perpendicular to a north-south base line. Sample locations are plotted on figure 7 and analytical results are given in table 5. Each sample was composed of approximately 3 kilograms of chips 3-6 cm across. Analytical results from each sample are plotted at the middle of each sample zone as shown in figure 7.

In addition, 25 composite chip samples were collected throughout the area from mineralized and altered zones. Analytical results are listed in table 6.

Distribution maps for copper, lead, and zinc are presented in figures 8, 9, and 10.

Core sampling

Representative samples 5 cm long were picked from different places along each drill core. All samples were split, one-half retained, and one-half submitted for analysis. Some apparently barren rocks were analyzed to check background contents of the rocks as well as to detect any mineralization that could not be observed in the hand specimen. Mineralized and altered zones were also sampled at various intervals. The analytical data are listed in tables 7 and 8. Mineralized

EXPLANATION

al	SILT, SAND, AND GRAVEL
r	RHYOLITE DIKE
m	METAPORPHYRITIC MAFIC DIKE
qt	QUARTZ VEINS
g	GOSSAN
if	IRON FORMATION
sf	METAFELSIC ROCK, RICH IN SERICITE AND LATE POTASSIUM FELDSPAR AND QUARTZ
cs	CHLORITE SCHIST, CONTAINING ELONGATED BLEBS RICH IN EPIDOTE
cso	CHLORITE SCHIST, OXIDIZED AND SERICITIZED

·ecambrian (bracket: if, sf, cs, cso)

- GEOLOGIC CONTACT, DASHED WHERE INFERRED
- LATERAL FAULTS, SHOWING DIRECTION OF MOVEMENT
- 20 — OVERTURNED ANTICLINE, SHOWING DIRECTION OF DIP OF LIMBS AND PLUNGE
- 50 — STRIKE AND DIP OF FOLIATION
- STRIKE OF VERTICAL FOLIATION
- 22 — STRIKE AND DIP OF JOINT
- 80 — STRIKE AND PLUNGE OF LINEATION
- SHEARED ROCK
- FAULT BRECCIA
- OPEN PIT
- Mh-4 — LOCATION AND VERTICAL PROJECTION OF DRILL HOLE
- + 0.0 560N — GEOCHEMICAL STATION ALONG BASE LINE
- COPPER–STAINED AREA
- DRAINAGE
- CULTIVATED LAND
- UNPAVED ROAD

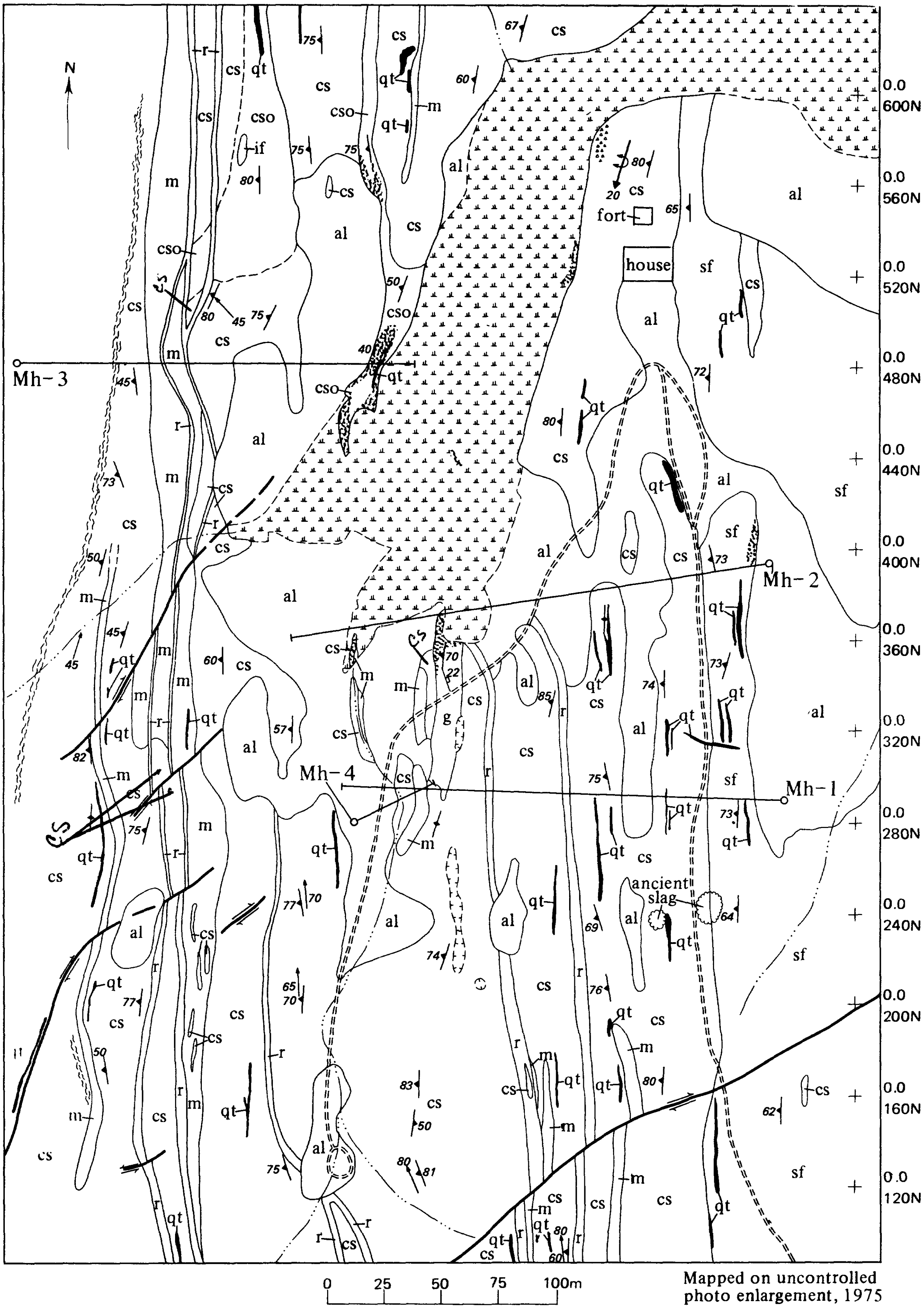

Figure 2.–Geologic map of Wadi Mandahah ancient mine.

Table 1.--*Summary geologic log of diamond drill hole Mh 1*

From (meters)	To (meters)	Description
0.0	12.55	Quartz-sericite schist, limonitic
12.55	20.9	Porphyroblastic chloritic schist, limonitic
20.9	35.75	Oxidized chlorite schist
35.75	44.25	Brecciated quartz-sericite schist
44.25	48.9	Porphyroblastic quartz-chlorite schist
48.9	56.45	Quartz and K-spar-rich sericite schist; disseminated pyrite 2 percent
56.45	60.35	Quartz-chlorite schist; pyrite along fractures 5 percent
60.35	70.60	Quartz and K-spar-rich sericite schist
70.60	81.55	Quartz-chlorite schist
81.55	83.9	Quartz vein with minor K-spar
83.9	91.05	Porphyroblastic chlorite schist, fractured
91.05	100.02	Epidotized chlorite schist, fractured
100.02	106.0	Quartz-sericite chlorite schist
106.0	126.4	Chlorite-sericite schist; disseminated pyrite (1-5 percent)
126.4	132.20	Sericite schist rich in K-spar
132.20	138.3	Chlorite-sericite schist
138.3	141.15	Rhyolitic dike
141.15	154.0	Quartz-sericite schist
154.0	156.15	Mafic dike
156.15	158.65	Quartz-sericite schist
158.65	162.25	Quartz vein: disseminated pyrite (5-25 percent)
162.25	165.85	Quartz-sericite schist
165.85	167.95	Rhyolitic dike
167.95	169.10	Limonitic chlorite schist
169.10	171.95	Rhyolitic dike
171.95	184.15	Chlorite schist
184.15	191.85	Limonitic chlorite schist; minor pyrite
191.85	193.05	No core
193.05	194.45	Chlorite-sericite schist
194.45	199.95	Mafic dike
199.95	212.60	Chlorite schist

Table 2.--*Summary geologic log of diamond drill hole Mh 2*

From (meters)	To (meters)	Description
0.0	7.0	Limonitic quartz-sericite schist
7.0	20.8	Porphyritic chlorite-sericite schist
20.8	40.5	Chlorite-sericite schist enriched with K-spar; minor pyrite
40.5	69.6	Quartz-sericite schist; pyrite along fractures; minor magnetite
69.6	74.8	Chlorite-sericite schist enriched with K-spar; minor pyrite and magnetite
74.8	99.85	Quartz-chlorite-sericite schist; minor disseminated pyrite and magnetite
99.85	109.6	Mafic porphyritic dike
109.6	143.85	Quartz-chlorite-sericite schist; minor pyrite
143.85	146.60	Chlorite schist
146.60	170.70	Quartz-sericite-chlorite schist; disseminated pyrite
170.70	178.30	Porphyroblastic chlorite schist
178.30	181.20	Rhyolitic dike
181.20	200.25	Sericite schist; sulfides concentrated in a fracture at 184.90 m
200.25	203.40	Quartz-sericite schist
203.40	211.30	Chlorite schist
211.30	211.80	Mafic dike
211.80	214.95	Sericite schist rich in quartz and K-spar
214.95	220.65	Mafic dike
220.65	229.65	Quartz-chlorite-sericite schist; pyrite and carbonate in the fractures
229.65	242.00	Oxidized rock; traces of malachite and fresh pyrite
242.00	244.00	Sericite-chlorite schist; 3 percent sulfides at 243.75 m (pyrite, galena, and sphalerite)
244.00	245.05	Chlorite schist
245.05	249.15	Mafic dike
249.15	265.60	Chlorite schist
265.60	284.50	Sericite-chlorite schist with disseminated pyrite

Table 3.--*Summary geologic log of diamond drill hole Mh 3*

From (meters)	To (meters)	Description
0.0	19.15	Porphyroblastic chlorite schist, slightly oxidized
19.15	41.40	Quartz-feldspathic-chlorite schist; minor pyrite; at base the rock is highly sheared and altered
41.40	44.80	Quartz-chlorite schist rich in K-spar
44.80	52.80	Quartz-chlorite schist; minor pyrite
52.80	59.10	Quartz-sericite-chlorite schist; minor pyrite
59.10	60.10	Blackened milky quartz
60.10	78.40	Porphyroblastic quartz-chlorite schist
78.40	83.55	Rhyolitic dike
83.55	86.80	Felsic rock rich in quartz and K-spar
86.90	94.0	Porphyroblastic quartz-chlorite schist
94.0	95.95	Rhyolitic dike
95.95	97.20	Porphyroblastic quartz-chlorite schist
97.20	97.55	No core
97.55	99.55	Porphyroblastic quartz-chlorite schist
99.55	159.15	Massive chloritic rock
159.15	160.45	Quartz-sericite-chlorite schist; pyrite (20 percent)
160.45	175.50	The same as above; no pyrite
175.50	184.8	Quartz-chlorite-schist; pyrite along cleavage planes
184.8	188.45	Mafic dike
188.45	192.75	Quartz-chlorite-sericite schist
192.75	204.70	Highly silicified sericite schist
204.70	210.10	Brecciated chlorite schist
210.10	218.30	Quartz sericite schist
218.30	223.15	Rhyolitic dike
223.15	234.45	Quartz-sericite-chlorite schist, minor pyrite

Table 4.--*Summary geologic log of diamond drill hole Mh 4*

From (meters)	To (meters)	Description
0.0	3.57	Covers
3.57	14.7	Oxidized chlorite schist with oxides and malachite
14.7	20.65	Chlorite schist with minor pyrite
20.65	26.6	Quartz-feldspathic-chlorite schist
26.6	30.85	Fine aggregates with pyrite
30.85	34.15	Quartz-sericite-chlorite schist
34.15	35.10	Porphyritic mafic dike
35.10	44.0	Quartz-sericite-chlorite schist
44.0	51.3	Chlorite schist with quartz and epidote rich blebs
51.3	58.35	Quartz-feldspathic-chlorite schist
58.35	61.2	Prophyritic mafic dike
61.2	66.70	Quartz-feldspathic-chlorite schist with minor sulfides at 61.55 m; 2 cm of massive sulfides (60 percent)
66.70	74.0	Quartz-chlorite schist, slightly oxidized and pyritiferous
74.0	74.15	Gouge
74.15	77.25	Silicified rock
77.25	77.35	Fine aggregate
77.35	81.3	Silicified rock
81.3	84.3	Fine aggregate
84.3	85.05	Silicified rock
85.05	89.65	Quartz-chlorite schist
89.65	93.3	Rhyolitic dike
93.3	94.55	Massive quartz-feldspathic-chlorite schist
94.55	96.65	Porphyritic mafic dike
96.65	100.0	Quartz-feldspathic-chlorite schist
100.0	101.6	Porphyritic mafic dike
101.6	109.10	Quartz-chlorite schist; disseminated pyrite
109.10	111.4	Rhyolitic dike
111.4	144.25	Quartz
144.25	148.2	Porphyritic mafic dike
148.2	152.9	Rhyolitic dike
152.9	155.85	Quartz-chlorite schist

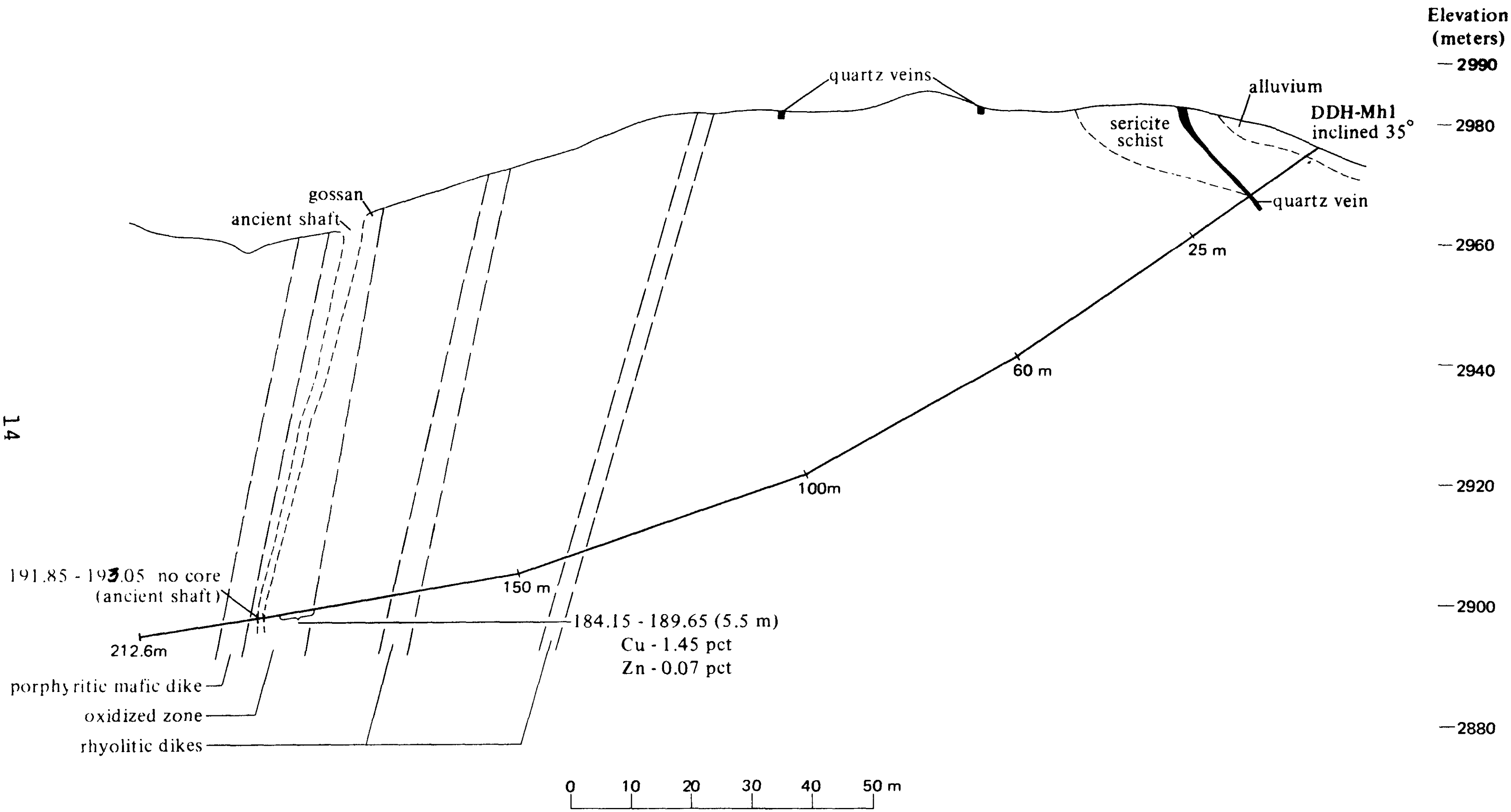

Figure 3.–Cross section of Wadi Mandahah drill hole Mh 1. Section looking north. Unless otherwise identified, country rock is chlorite schist.

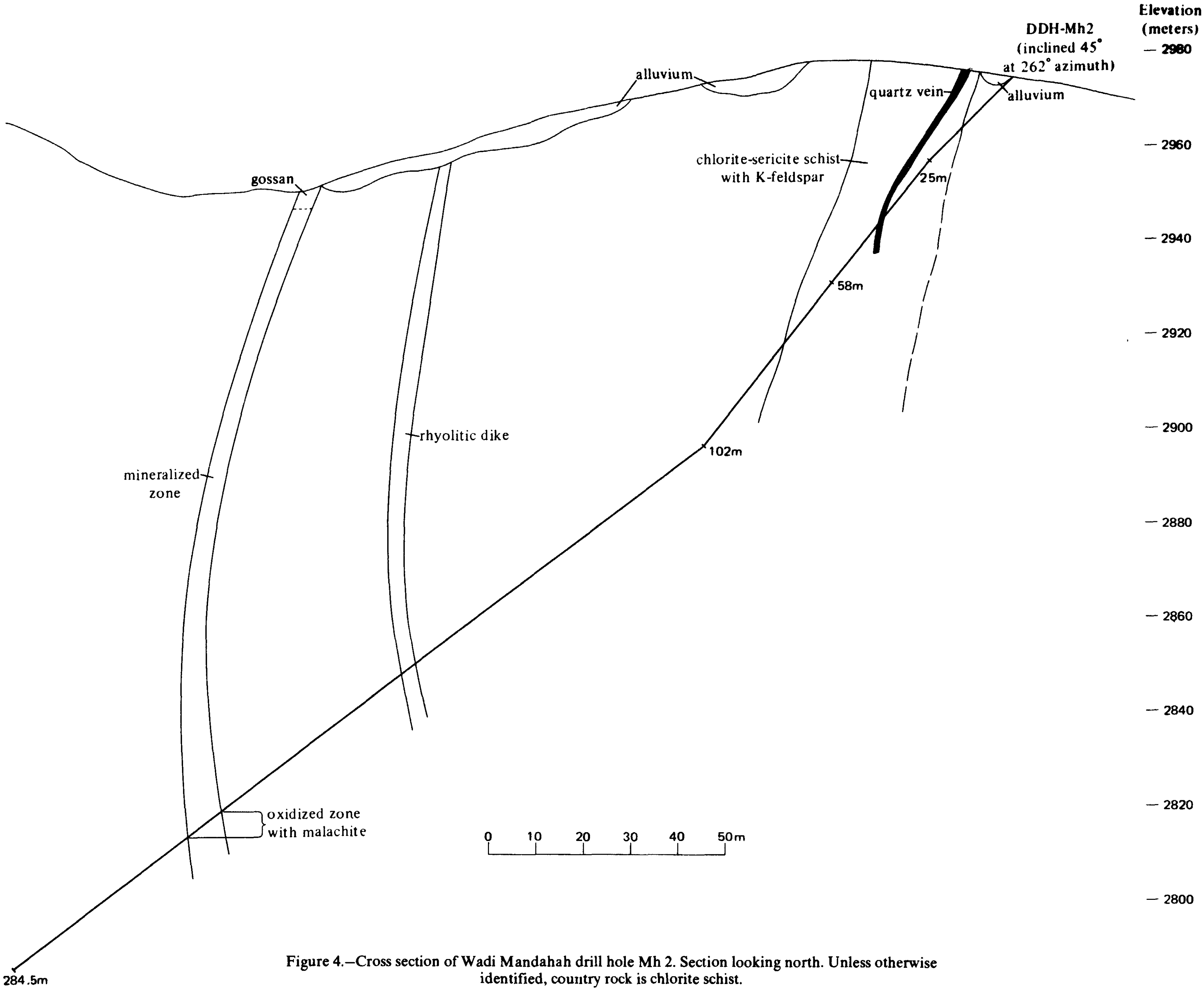

Figure 4.—Cross section of Wadi Mandahah drill hole Mh 2. Section looking north. Unless otherwise identified, country rock is chlorite schist.

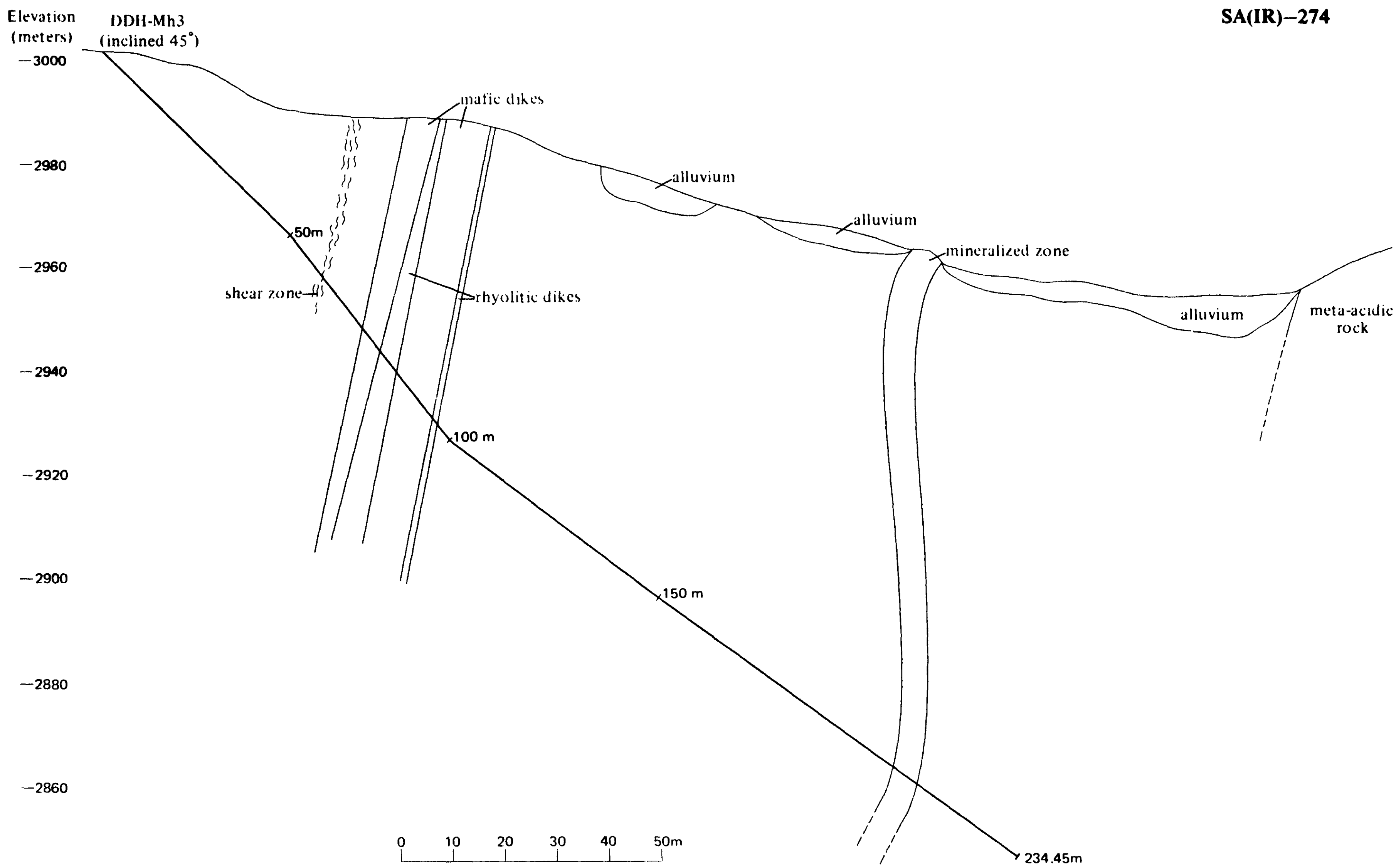

Figure 5.—Cross section of Wadi Mandahah drill hole Mh 3. Section looking north. Unless otherwise identified, country rock is chlorite schist.

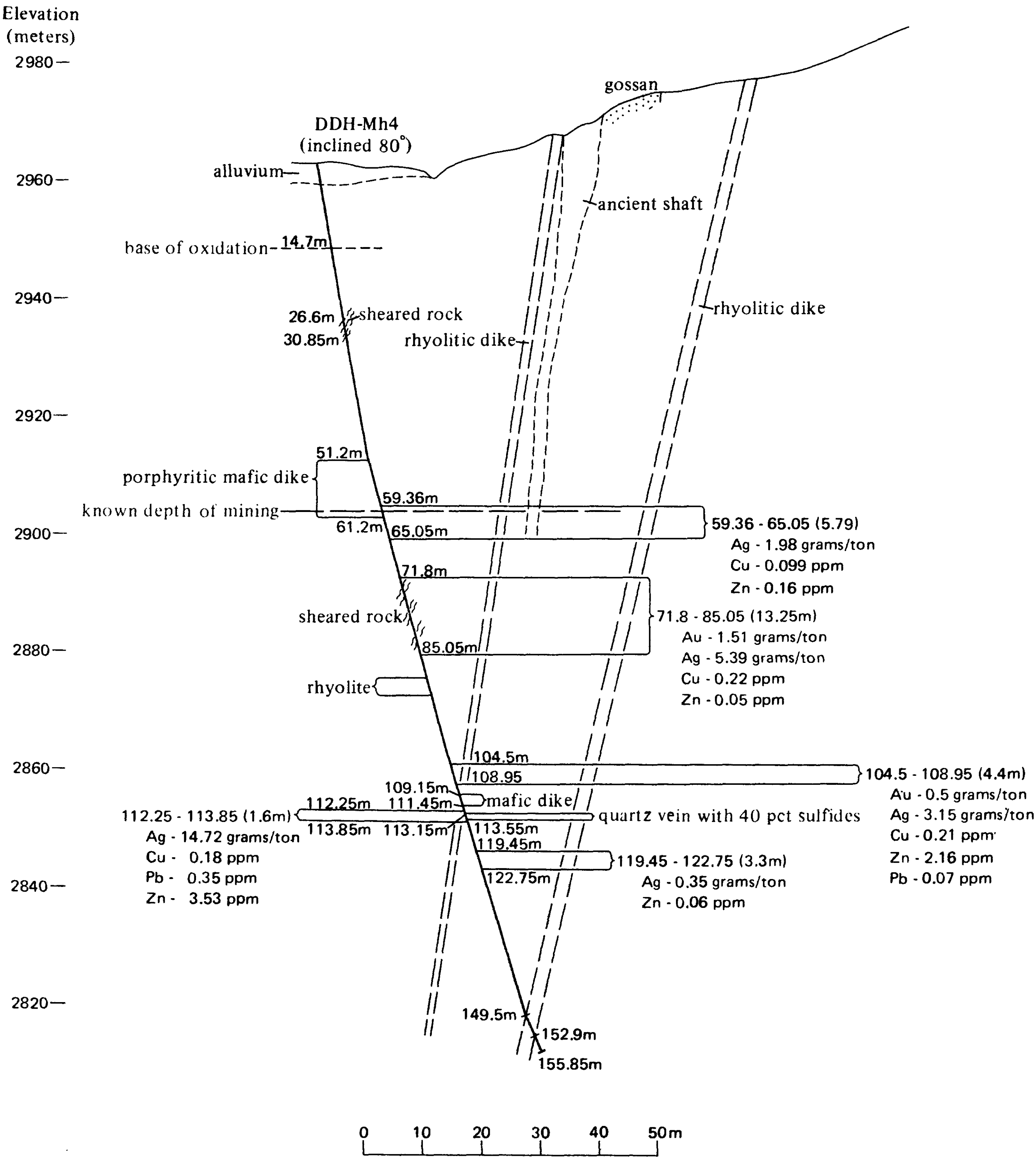

Figure 6.—Cross section of Wadi Mandahah drill hole Mh 4. Section looking north. Unless otherwise identified, country rock is chlorite schist.

zones and the mean value of anomalous elements of each zone in drill holes Mh 1 and Mh 4 are listed in the cross sections (figs. 3 and 6 respectively).

The sulfide bodies at depth are very narrow compared to the width of the gossan at the surface. The sulfides are found in the highly siliceous parts of the chlorite schist and are located in shear planes rather than in the quartz-rich zones. The main sulfides are pyrite, which forms large euhedral cubes (1 cm^3), and minor amounts of chalcopyrite and galena. These pyrite cubes formed within the chlorite and changed the orientation of the chlorite flakes. All sulfides were formed contemporaneously although it is evident that pyrite started to crystallize first.

Discussion

The country rocks do not contain anomalous concentrations of base metals, whereas the gossans are enriched in copper and zinc. Copper and zinc are highly concentrated at the surface, but are sparse at depth and may have migrated upward along cleavage and shear planes. The mineralization is restricted to the central and eastern shear zones.

Allcott (written commun., 1977) made surface geochemical studies at several prospects in the Wadi Bidah district just to the east and noted that copper and zinc are not significant elements for geochemical investigation; that is, areas enriched in these elements are not necessarily metallized at depth. Iron/magnesium ratios of more than 5 and enrichment in lead, silver, barium, nickel, gold, and manganese are thought by Allcott to be better indicators.

The four holes drilled in the Wadi Mandahah area intersected only very minor sulfides in rocks beneath the gossans. Furthermore, no sulfide was seen in cores from beneath the areas that show conspicuous copper stains, even from below the northern part of the gossan, which contains abundant malachite but no limonite. Other areas rich in malachite and slightly limonitic are not mineralized at depth, and apparently the limonite formed as a result of oxidation of iron-rich minerals of the country rocks, for example chlorite, and not of sulfides.

Surface indications of mineralization at the Wadi Mandahah ancient mine--gossan and secondary enrichment of copper and zinc--are not conspicuous. The gossan is not rich enough in oxidized sulfides to suggest that massive sulfide deposits exist at depth, and surficial copper concentrations in the area do not seem to extend downward. Worl (1978) found the same situation in the Umm al Khabath area, where in several shallow trenches across copper-rich zones the metal content of samples collected below the surface was very low.

Table 5.--*Analytical data on surface composite chip samples along geochemical grid at Wadi Mandahah mine Atomic absorption analyses by DGMR laboratory*
[(-), not detected]

Sample number	Copper (ppm)	Lead (ppm)	Zinc (ppm)	Manganese (ppm)	Nickel (ppm)
101110	140	35	240	1,450	200
101102	45	165	210	450	55
101102	45	50	140	1,550	33
101103	140	33	250	700	43
101104	285	145	1,230	850	33
101105	110	50	740	1,600	33
101106	210	45	210	1,060	43
101107	140	45	350	1,050	33
101108	35	50	100	640	43
101109	135	28	1,590	970	43
101110	65	55	140	300	50
101111	20	35	320	425	40
101112	105	45	320	1,130	-
101113	275	270	590	1,170	43
101114	765	80	680	590	43
101115	240	60	280	1,150	25
101116	715	30	280	880	43
101117	855	25	430	1,030	23
101118	190	35	520	2,000	25
101119	70	240	260	550	25
101120	40	300	390	1,290	43
101121	225	55	240	1,450	55
101122	240	20	480	740	43
101123	520	30	560	1,700	43
101124	275	-	310	1,150	50
101125	715	-	220	970	43
101126	135	-	1,000	1,450	58
101127	70	96	270	1,350	43
101128	285	615	520	1,550	35
101129	1,000	35	210	425	40
101130	655	-	470	985	65
101131	895	-	700	1,070	45
101132	740	-	430	1,300	25
101133	1,350	-	470	36	16
101134	3,000	45	260	1,020	36

Table 5.--*Analytical data on surface composite chip samples along geochemical grid at Wadi Mandahah mine. Atomic absorption analyses by DGMR laboratory*
[(-), not detected] [continued]

Sample number	Copper (ppm)	Lead (ppm)	Zinc (ppm)	Manganese (ppm)	Nickel (ppm)
101135	650	35	430	1,850	45
101136	240	275	470	2,050	45
101137	650	30	390	1,290	45
101138	200	40	250	490	40
101139	110	45	470	1,850	55
101140	3,700	40	590	2,600	25
101141	360	545	910	6,200	25
101142	24,400	30	2,050	1,400	-
101143	1,000	30	530	1,450	-
101144	180	105	880	1,700	-
101145	300	35	350	1,750	25
101146	2,850	35	890	1,470	40
101147	1,000	50	260	860	45
101148	2,000	50	730	1,050	25
101149	230	50	290	1,700	25
101150	1,050	45	180	1,450	25
101151	1,270	30	260	970	-
101152	1,500	65	330	460	-
101153	20,000	50	2,410	1,180	20
101154	240	50	280	1,340	20
101155	3,200	30	500	1,080	20
101156	9,400	20	1,190	790	-
101157	720	30	140	820	-
101158	1,500	30	180	340	-
101159	470	30	280	1,110	-
101160	390	110	430	850	-
101161	870	60	320	910	-
101162	200	30	100	230	25
101163	6,750	45	1,070	530	25
101164	240	35	40	320	-
101165	100	65	170	1,070	-
101166	210	50	330	720	-
101167	280	50	180	560	-
101168	220	330	480	750	-
101169	2,130	130	280	610	-

Table 5.--*Analytical data on surface composite chip samples along geochemical grid at Wadi Mandahah mine Atomic absorption analyses by DGMR laboratory*
[(-), not detected] [continued]

Sample number	Copper (ppm)	Lead (ppm)	Zinc (ppm)	Manganese (ppm)	Nickel (ppm)
101170	840	170	390	1,110	-
101171	250	35	100	450	-
101172	330	35	240	390	-
101173	480	35	100	160	-
101174	690	35	100	360	-
101175	100	65	170	1,070	-
101176	210	50	330	720	-
101177	280	50	180	560	-
101178	1,120	330	480	750	-
101179	2,130	130	280	610	-
101180	25,250	90	670	360	-
101181	550	75	820	770	-
101182	6,900	60	1,130	880	-
101183	1,050	60	120	315	-
101184	1,600	-	380	330	25
101185	140	50	200	1,550	25
101186	130	75	710	1,850	25
101187	1,775	35	390	1,160	75
101188	930	35	200	950	-
101189	330	35	420	1,440	-
101190	4,525	100	750	880	-
101191	350	50	390	380	-
101192	2,850	30	720	1,100	-
101193	90	30	85	420	-
101194	75	30	290	1,100	-
101195	65	65	180	1,270	-
101196	210	50	410	820	35
101197	155	60	150	1,030	-
101198	260	25	160	880	-
101199	3,400	30	720	1,070	-
101200	800	35	410	1,300	-
101201	340	35	790	1,200	25
101202	480	35	260	560	-
101203	420	35	230	910	-
101204	1,200	25	210	500	20

Table 5.--*Analytical data on surface composite chip samples along geochemical grid at Wadi Mandahah mine Atomic absorption analyses by DGMR laboratory*
[(-), not detected] [continued]

Sample number	Copper (ppm)	Lead (ppm)	Zinc (ppm)	Manganese (ppm)	Nickel (ppm)
101205	60	15	100	1,070	25
101206	110	25	150	1,400	55
101207	75	15	240	1,360	-
101208	150	15	200	1,450	-
101209	160	15	160	1,000	-
101210	290	-	300	1,100	-
101211	750	30	380	1,300	-
101212	170	30	360	600	-
101213	470	25	470	1,460	-
101214	90	15	75	710	-
101215	35	10	130	1,080	-
101216	33	-	110	770	-
101217	110	-	670	1,100	-
101218	38	-	110	1,360	35
101219	35	-	200	1,450	25
101220	180	-	75	730	-
101221	540	170	820	1,070	-
101222	140	310	310	710	-
101223	75	-	360	1,060	-
101224	40	-	170	1,200	-
101225	25	25	130	1,130	-
101226	75	-	130	880	25
101227	35	600	150	1,000	-
101228	100	120	590	1,500	-
101229	50	-	100	970	-
101230	50	-	110	1,030	-
101231	255	-	180	900	-
101232	615	-	810	1,040	-
101233	80	-	520	740	-
101234	90	-	230	1,000	-
101235	33	-	180	875	-
101236	85	-	190	1,340	-
101237	40	-	90	570	95
101238	80	-	250	1,030	-
101239	35	-	100	970	-

Table 5.--*Analytical data on surface composite chip samples along geochemical grid at Wadi Mandahah mine Atomic absorption analyses by DGMR laboratory*
[(-), not detected] [continued]

Sample number	Copper (ppm)	Lead (ppm)	Zinc (ppm)	Manganese (ppm)	Nickel (ppm)
101240	80	-	190	970	-
101241	270	-	230	1,310	25
101242	80	35	120	490	-
101243	190	170	550	460	-
101244	90	10	240	1,040	-
101245	60	-	110	820	-
101246	50	-	130	570	-
101247	35	-	110	910	-
101248	30	-	90	710	-
101249	90	15	170	1,170	-
101250	80	-	440	2,300	-
101251	20	-	20	465	-
101252	25	-	40	690	-
101253	290	780	970	660	-
101254	60	-	270	2,300	-
101255	50	-	150	890	-
101256	15	-	-	180	-
101257	10	-	-	250	-
101258	85	45	300	1,400	25
101259	50	10	35	600	-
101260	45	-	140	1,200	-
101261	50	-	55	450	-
101262	60	-	140	970	-
101263	265	-	340	2,300	-
101264	40	-	60	420	-
101265	13	-	30	150	-
101266	90	-	390	830	-
101267	70	-	140	850	-
101268	45	-	90	1,100	-
101269	60	-	3(0	1,200	-
101270	30	-	40	410	-
101271	85	-	440	2,000	-
101272	45	-	80	930	-
101273	70	-	50	450	-
101274	90	-	50	380	-

Table 6.--*Analytical data on surface composite chip samples across mineralized and altered zones at Wadi Mandahah mine. Atomic absorption analyses by DGMR laboratory.*

[(-), not detected]

Sample number	Copper (ppm)	Lead (ppm)	Zinc (ppm)	Manganese (ppm)	Nickel (ppm)
101275	3475	35	410	720	55
101276	7125	135	810	1,100	70
101277	8000	45	590	410	55
101278	3525	65	690	1,500	65
101279	1475	25	970	2,500	55
101280	575	-	160	260	65
101281	175	-	50	280	25
101282	7800	-	1,080	1,750	25
101283	100	15	140	2,300	45
101234	135	-	110	950	25
101285	10,000	-	1,080	870	35
101286	12,000	-	1,800	1,400	35
101287	3,400	-	730	260	65
101288	12,500	-	860	310	35
101289	9,000	45	1,140	680	45
101290	15,500	45	1,300	430	45
101291	48,500	13	6,500	2,100	116
101292	4,100	13	920	1,300	25
101293	2,900	15	970	760	-
101294	3,080	-	1,060	660	-
101295	16,500	-	2,070	310	25
101296	13,800	-	1,400	1,180	45
101297	425	-	170	520	35
101298	2,250	-	240	200	-
101299	250	-	60	185	50

Table 7.--*Analytical data on core samples from drill hole Mh-1. Atomic absorption analyses by DGMR laboratory.* [(-), not detected]

Sample number	Interval (meters) From	To	Gold (ppm)	Silver (ppm)	Copper (percent)	Lead (percent)	Zinc (percent)
101502	94.00	94.05	-	-	0.008	-	0.14
101503	99.2	99.25	-	0.3	0.073	-	0.021
101504	120.00	121.45	-	-	0.073	-	0.035
101505	125.65	126.00	-	-	0.002	-	0.008
101507	142.65	142.30	-	-	0.083	0.002	0.063
101508	155.10	155.15	-	48	0.073	-	0.240
101509	195.45	195.50	-	0.385	0.004	-	0.200
101510	160.75	160.80	-	0.35	0.006	-	0.140
101513	172.10	172.15	-	0.30	0.003	0.001	0.031
101514	184.15	185.55	2.5	11.5	3.125	0.001	0.045
101515	186.15	189.65	0.56	30	0.775	0.001	0.080

Table 8.--*Analytical data on core samples from drill hole Mh-4. Atomic absorption analyses by DGMR laboratory.*
[(-), not detected]

Sample number	Interval (meters) From	To	Gold (ppm)	Silver (ppm)	Copper (percent)	Lead (percent)	Zinc (percent)
101567	59.36	60.36	-	1.16	0.0045	0.002	0.025
101568	60.36	61.00	-	0.92	0.004	-	0.064
101562	61.00	61.55	0.1	1.08	0.0475	-	0.025
101569	61.55	62.05	-	0.88	0.0475	-	0.043
101570	62.05	62.85	0.64	1.24	0.06	-	0.200
101571	62.85	63.50	0.64	3.80	0.2475	0.015	0.82
101563	63.50	63.95	2.22	3.88	0.026	-	0.82
101572	63.95	64.45	0.64	1.76	0.13	0.0015	0.038
101573	64.45	65.05	1.11	3.48	0.375	0.0018	0.100
101574	71.80	72.8	0.14	1.76	0.0165	0.0035	0.041
101575	72.8	73.45	-	0.76	0.012	-	0.01
101576	73.45	74.00	-	1.4	0.011	0.003	0.079
101577	74.00	75.05	0.1	1.0	0.055	0.0015	0.025
101578	75.05	75.90	0.07	9.80	0.1475	-	0.029
101579	75.90	77.25	0.1	23.6	0.03	-	0.034
101580	77.25	78.35	0.1	7.4	0.155	0.002	0.07
101581	78.35	80.00	0.54	2.12	0.300	0.0015	0.023
101582	80.00	80.75	0.10	0.92	0.14	0.15	0.042
101583	80.75	81.30	0.32	0.92	0.245	0.002	0.043
101584	81.36	83.70	7.28	5.0	0.405	6.004	0.078
101585	83.70	85.05	0.64	1.76	0.565	0.0033	0.048
101586	104.50	104.75	-	0.88	0.26	0.011	0.500
101587	104.75	105.3	0.64	1.24	0.475	0.001	0.085
101588	105.3	106.3	1.0	1.12	0.04	0.003	0.270
101589	106.3	106.9	0.86	2.24	0.022	0.02	0.200
101590	106.9	107.5	0.32	4.68	0.238	0.020	5.200
101591	107.5	107.8	0.22	7.00	0.425	0.032	6.300
101592	107.8	108.6	-	2.32	0.400	0.302	1.900
101593	108.6	108.95	0.14	12.4	0.088	0.06	8.00
101594	112.25	113.15	0.14	16.40	0.048	0.425	2.00
101565	113.15	113.55	0.32	21.6	0.62	0.46	9.60
101595	113.55	113.85	-	0.5	0.005	0.002	0.102
101596	119.45	120.45	-	0.2	0.0027	-	0.027
101566	120.45	120.70	-	0.32	0.0026	-	0.155
101597	120.70	121.50	0.16	0.44	0.0027	0.004	0.085
101598	121.50	121.85	-	0.20	0.006	-	0.054
101599	121.85	122.75	-	0.52	0.006	-	0.060

The high copper and zinc values on the surface are possibly the result of migration of these metals in percolating water and deposition at the surface as secondary carbonates. However, these anomalous values might indicate a concentration of these metals somewhere else in the area; the metals could have migrated only a few meters or more than a hundred meters.

GEOPHYSICAL SURVEY

by

H. M. Merghelani

A self-potential (SP) unit was used in the survey. An ABEM (type 5241) Turam electromagnetic (EM) unit with operating frequencies of 220 hertz and 660 hertz and a 20 m coil separation was used in making the EM observations. A primary field transmitter cable of 2 km length was laid parallel to the general northerly trends of the geologic formation. All measurements were taken along traverses 40 m apart with 20 m station intervals. The traverses were approximately 400 m long crossing the mine area. A hand level and tape were used to lay out all stations and traverses.

The SP data indicate two distinctive anomalies of shallow origin (fig. 11):

(1) A maximum potential of about -100 mv was recorded over an area of about 120 by 60 m, which coincides with the area of ancient mine workings (fig. 11).

(2) In the northern part of the mine area, a maximum potential of -140 mv was recorded over an area of about 40 by 40 m, which may reflect mine dump material (fig. 11).

EM data indicate a moderately high reduced-ratio anomaly that reaches a maximum of 1:1.35 at the south end of the ancient mine and that has apparent dimensions of 120 by 40 m. A weak reduced-ratio anomaly (1:1.10) following the general north-south trend of the geology is thought to reflect changes in conductivity in the zone of alteration associated with the mineral deposit (fig. 12).

For the main anomaly the depth was estimated by using profile 320 N and identifying the point where the slope starts to change; the depth estimate to the top of the conductor is about 35 m (fig. 13). For the northern SP anomaly, the depth to the top of the conductor was estimated to be about 23 m (fig. 14).

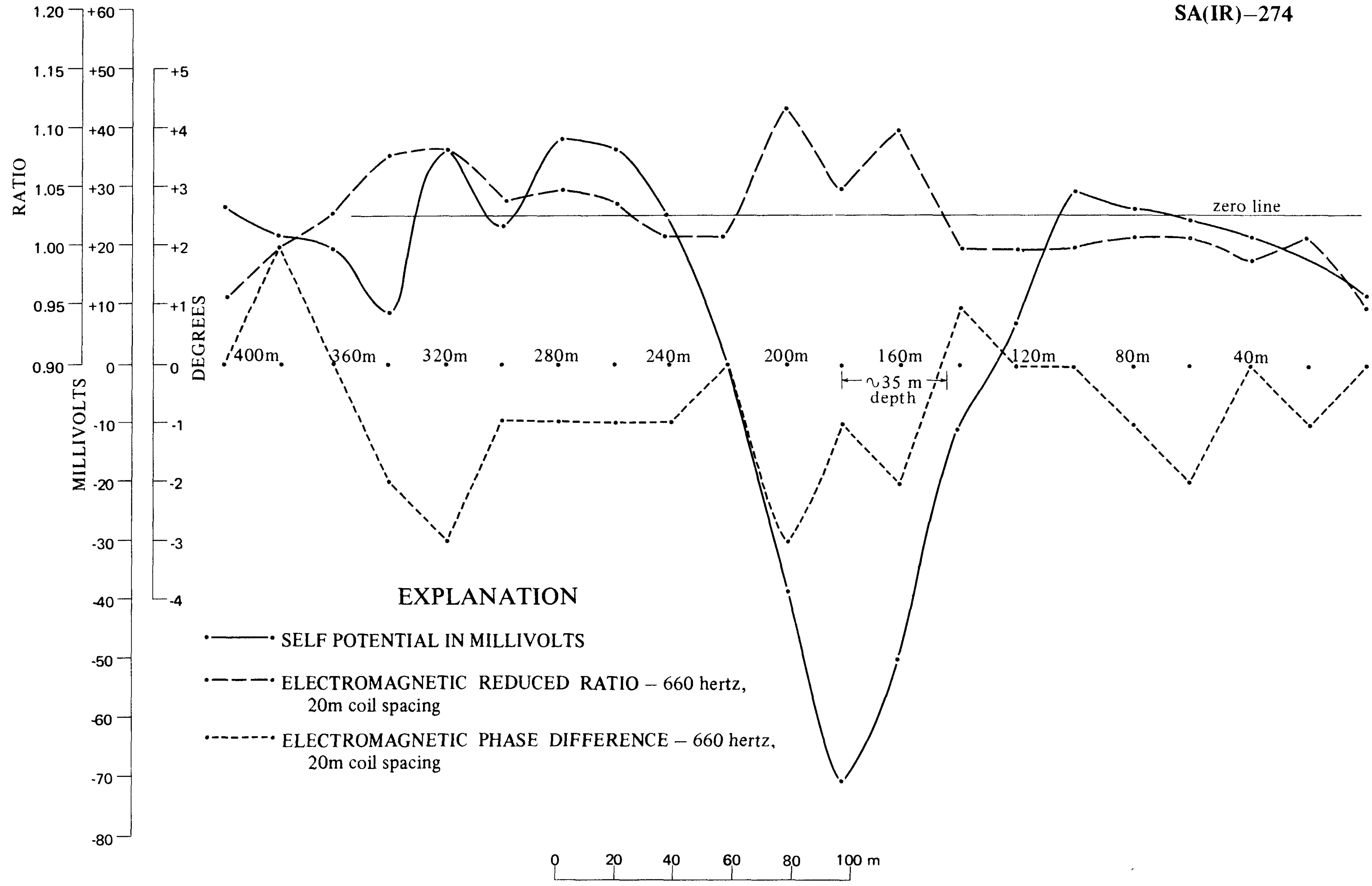

Figure 13.–Geophysical survey profile 320 N, Wadi Mandahah ancient mine.

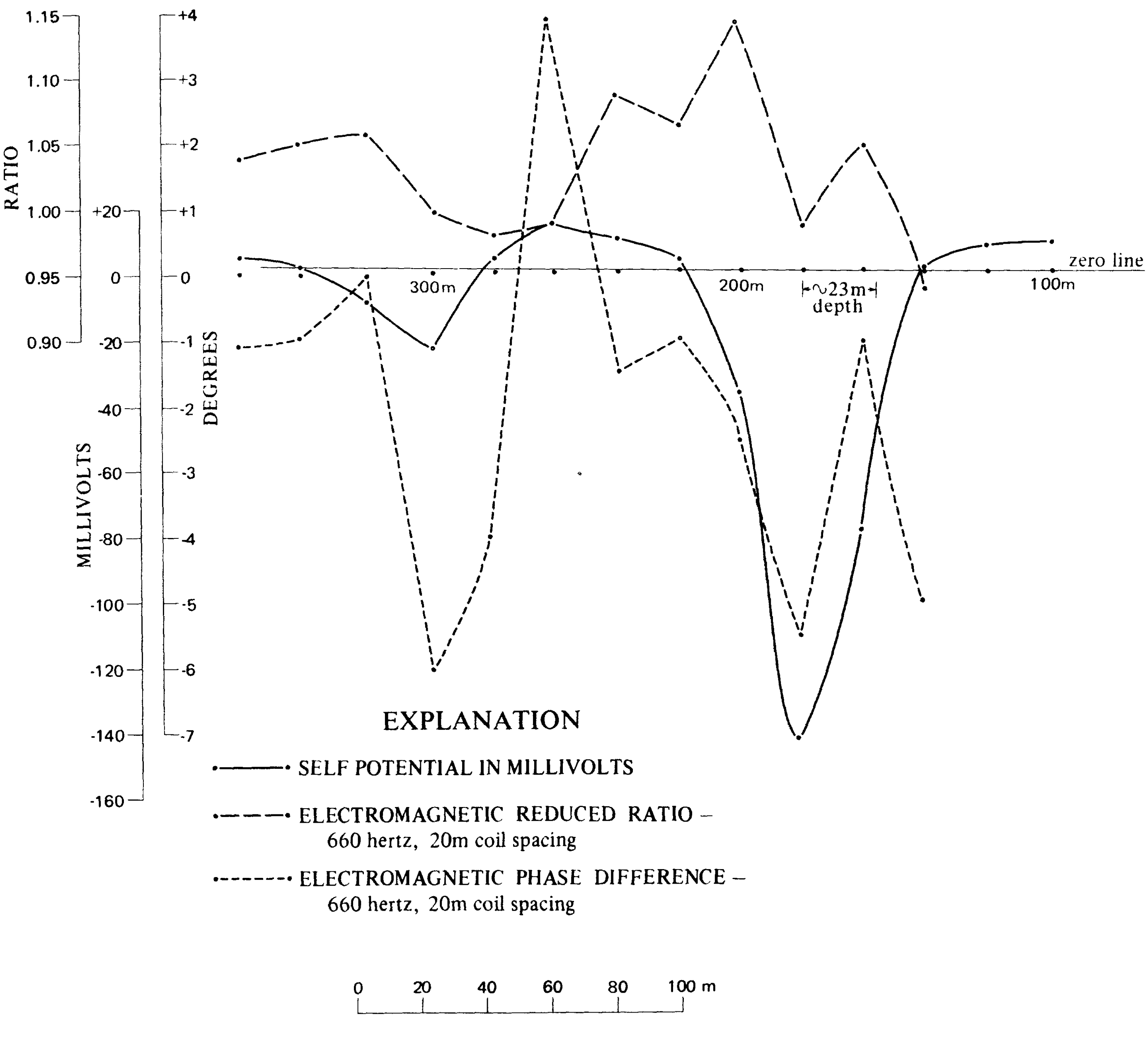

Figure 14.–Geophysical survey profile 600 N, Wadi Mandahah ancient mine.

CONCLUSIONS

The country rocks at the Wadi Mandahah ancient mine are mainly metavolcanics that are cut by granite intrusions, porphyritic mafic dikes, and dikes of diorite to quartz diorite and of rhyolite. Structurally, several periods of deformation are recognized. During uplift of the country rocks under north-south confining pressure, tight folds were deformed by ruptures and development of major faults in the north-south direction. Afterward, shearing along a north-south trend developed foliation and schistosity. Finally, a system of northwest- and northeast-trending conjugate faults was developed; these faults have slight displacements. Several generations of quartz were formed before, during, or after these tectonic events. The mineral deposits of Wadi Mandahah were formed after the first two tectonic events; minerals of the deposits are not deformed and are localized along shear planes and probably in the noses of folds.

The mineral deposits consist of pyrite, chalcopyrite, galena, and sphalerite, together with quartz, chlorite, sericite, and epidote. The sulfides formed by either hydrothermal processes or by segregation from the country rocks during regional metamorphism or possibly by a combination of these two processes. Hydrothermal processes are indicated in the eastern part of the area by the feldspar-rich zones, which are slightly sericitized and silicified. Several veins of massive and milky quartz also are mapped in this area. Erratically distributed stringers of euhedral sulfide crystals may have formed hydrothermally in low pressure zones along shear planes and at fold noses. This type of sulfide shows no sign of deformation and is posttectonic.

Originally disseminated sulfides may have been segregated during regional metamorphism. These sulfides are deformed, stretched, and smeared along the shear planes. Minor pyrite, chalcopyrite, and sphalerite also occur in some amygdules that are filled with epidote and quartz or with calcite. These sulfides were segregated from the metavolcanics and deposited in the amygdules.

BIBLIOGRAPHY

Brown, G.F., Jackson, R. O., Bogue, R. G., and Maclean, W. H., 1963, Geologic map of the southern Hijaz quadrangle, Kingdom of Saudi Arabia: U.S. Geological Survey Miscellaneous Geologic Investigation Map I-210A, scale 1:500,000

Earhart, R. C., and Mawad, M. M., 1970, Geology and mineral evaluations of the Wadi Bidah district, southern Hijaz quadrangle, Kingdom of Saudi Arabia: U.S. Geological Survey Open-file Report (IR)SA-119, 100 p.

Greenwood, W. R., 1975, Geology of the Jabal Ibrahim quadrangle, sheet 20/41 C, Kingdom of Saudi Arabia, with a section on Economic geology by R. G. Worl and W. R. Greenwood: Saudi Arabian Directorate General of Mineral Resources Geologic Map GM-22, scale 1:100,000.

Greenwood, W. R., Roberts, R. J., and Bagdady, A., 1974a, Mineral belts in western Saudi Arabia: Arab Conference on Mineral Resources, 2nd, 1974, Jiddah, Saudi Arabia, Conference Documents, Background Papers, Misc., p. 130-151.

Greenwood, W. R., Roberts, R. J., Kiilsgaard, T. H., Puffet, Willard, and Naqvi, I. M., 1974b, Massive sulfide deposits in the Wadi Bidah mining district, Kingdom of Saudi Arabia: Arab Conference on Mineral Deposits, 2nd, Jiddah, Conference Documents, Background Papers, Copper, p. 86-89.

Jackaman, Barry, 1972, Genetic and environmental factors controlling the formation of the massive sulphide deposits of Wadi Bidah and Wadi Wassat, Saudi Arabia: Saudi Arabian Directorate General of Mineral Resources Technical Record TR-1972-1, 244 p.

Mawad, M., 1975, Structural and mineralization studies of the Wadi Mandahah district: unpublished M.Sc thesis, King Abdul Aziz University, Institute for Applied Geology, Kingdom of Saudi Arabia, 112 p.

Metz, Karl, Ertl, V., Fehleissen, F., Litscher, H., and Petschnigg, H., 1971, The geology of the Aqiq-Ablah and Wadi Bidah-Mahawiyah area: Saudi Arabian Directorate General of Mineral Resources Technical Record TR-1971-2, 60 p.

Smith, C. W., 1964, Geologic report, Mahawiyah-Al Mashiga area: Saudi Arabian Directorate General of Mineral Resources open-file report 245, 5 p.

Worl, R. G., 1978, Evaluation of the Umm al Khabath copper prospect, Jabal Ibrahim quadrangle, sheet 20/41 C, Kingdom of Saudi Arabia: with a section on Geophysical investigations, by V. J. Flanigan and H. M. Merghelani: U.S. Geological Survey Open-file Report 78-521, (IR)SA-213, 42 p.

SA(IR)–274

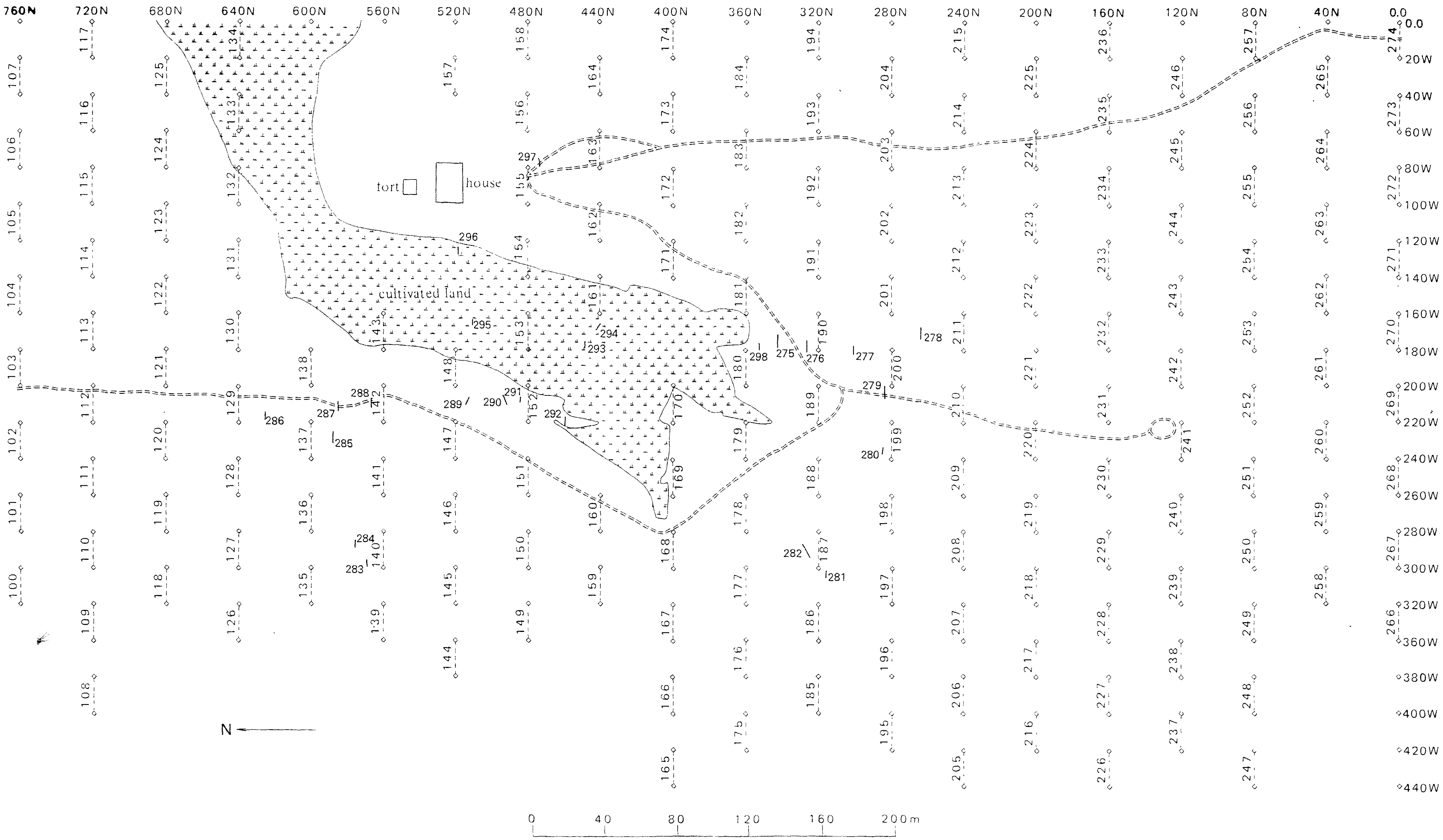

EXPLANATION

165 SAMPLE INTERVAL AND LAST THREE DIGITS OF SAMPLE NUMBERS IN 101000 SERIES

282\ LOCATION AND NUMBER OF CHIP SAMPLE FROM MINERALIZED ZONE

360N GEOPHYSICAL STATION

===== UNPAVED ROAD

Figure 7.--Geochemical base map of Wadi Mandahah ancient mine.

U.S. Geological Survey
Open-File Report 80-1262

SA(IR)–274

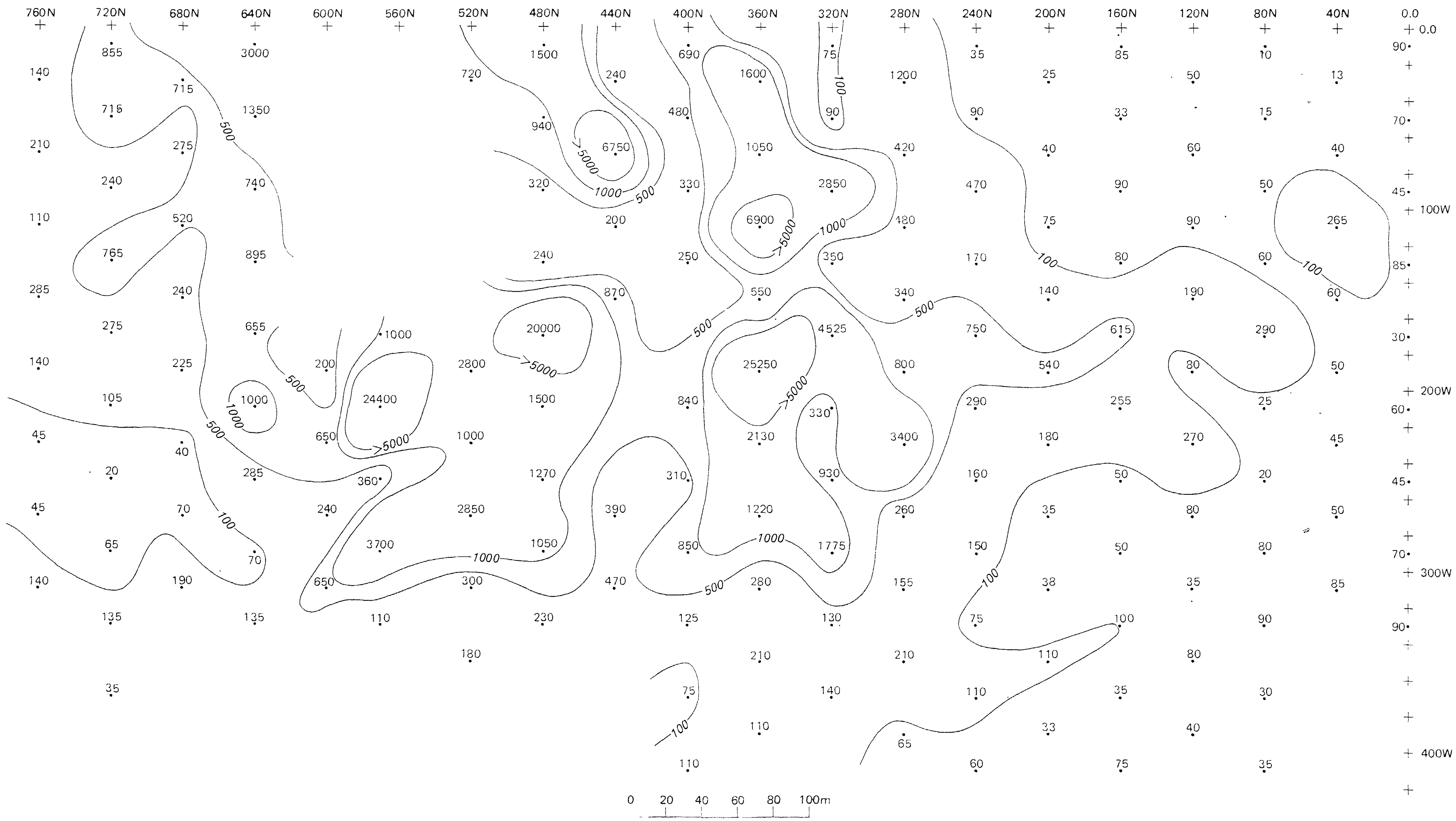

Figure 8.—Map showing distribution of copper in surface samples, Wadi Mandahah ancient mine. Contours are 100, 500, 1000, and 5000 parts per million.

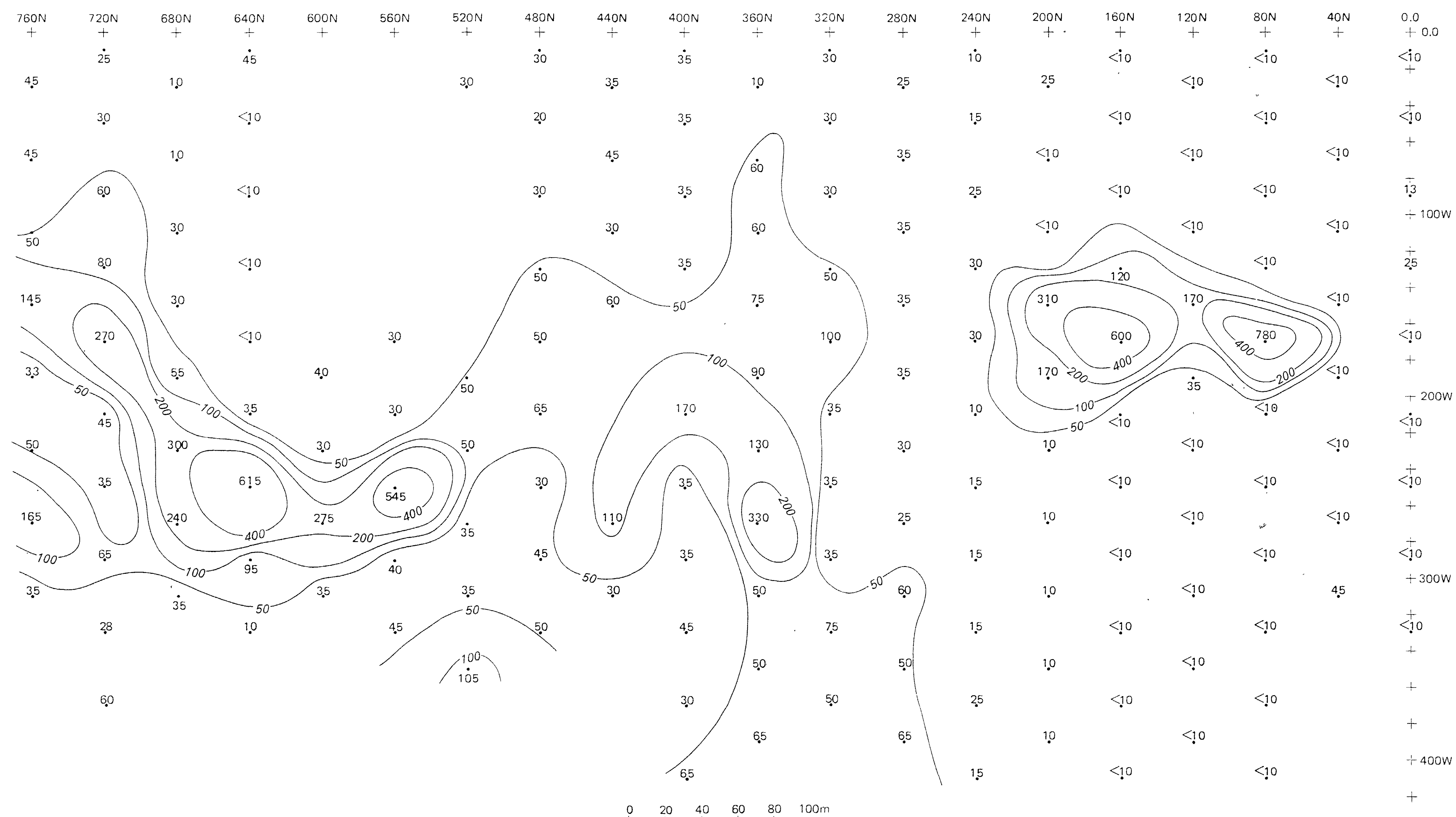

Figure 9.--Map showing distribution of lead in surface samples, Wadi Mandahah ancient mine. Contours are 50. 100. 200, and 400 parts per million.

SA(IR)-274

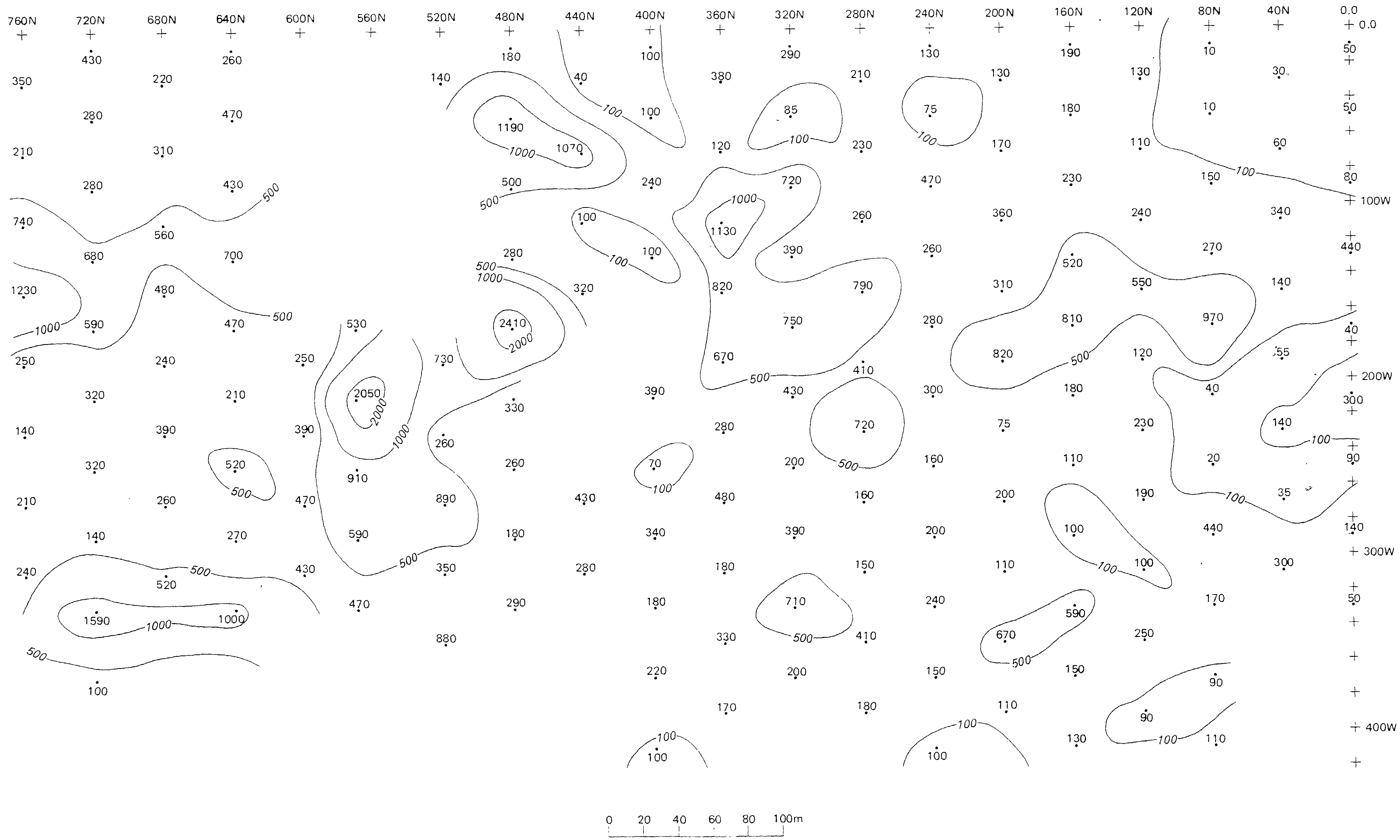

Figure 10.—Map showing distribution of zinc in surface samples, Wadi Mandahah ancient mine. Contours are 100, 500, 1000, and 2000 parts per million.

SA(IR)–274

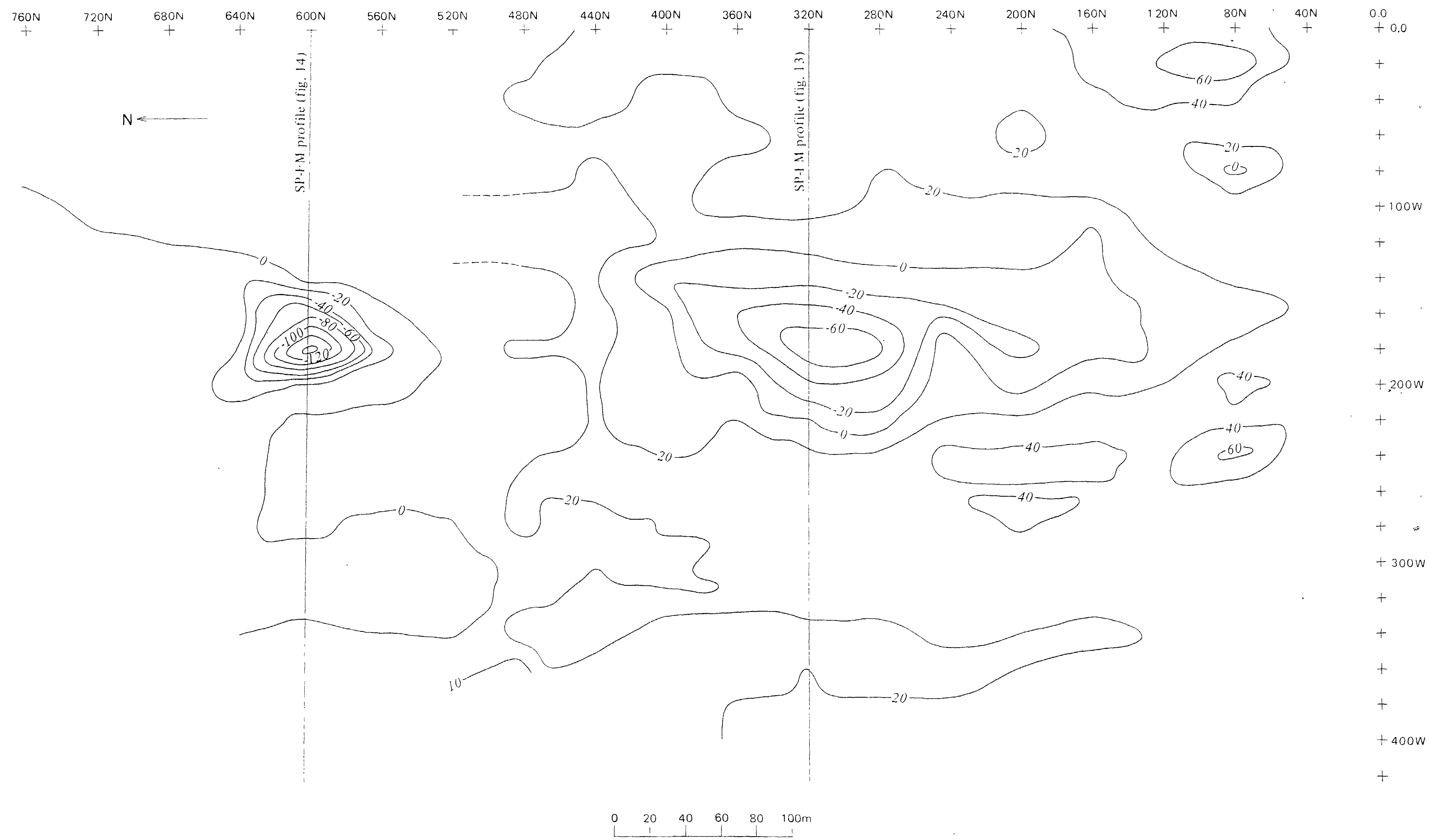

Figure 11.--Self-potential map of Wadi Mandahah ancient mine. Contour interval 20 mv.

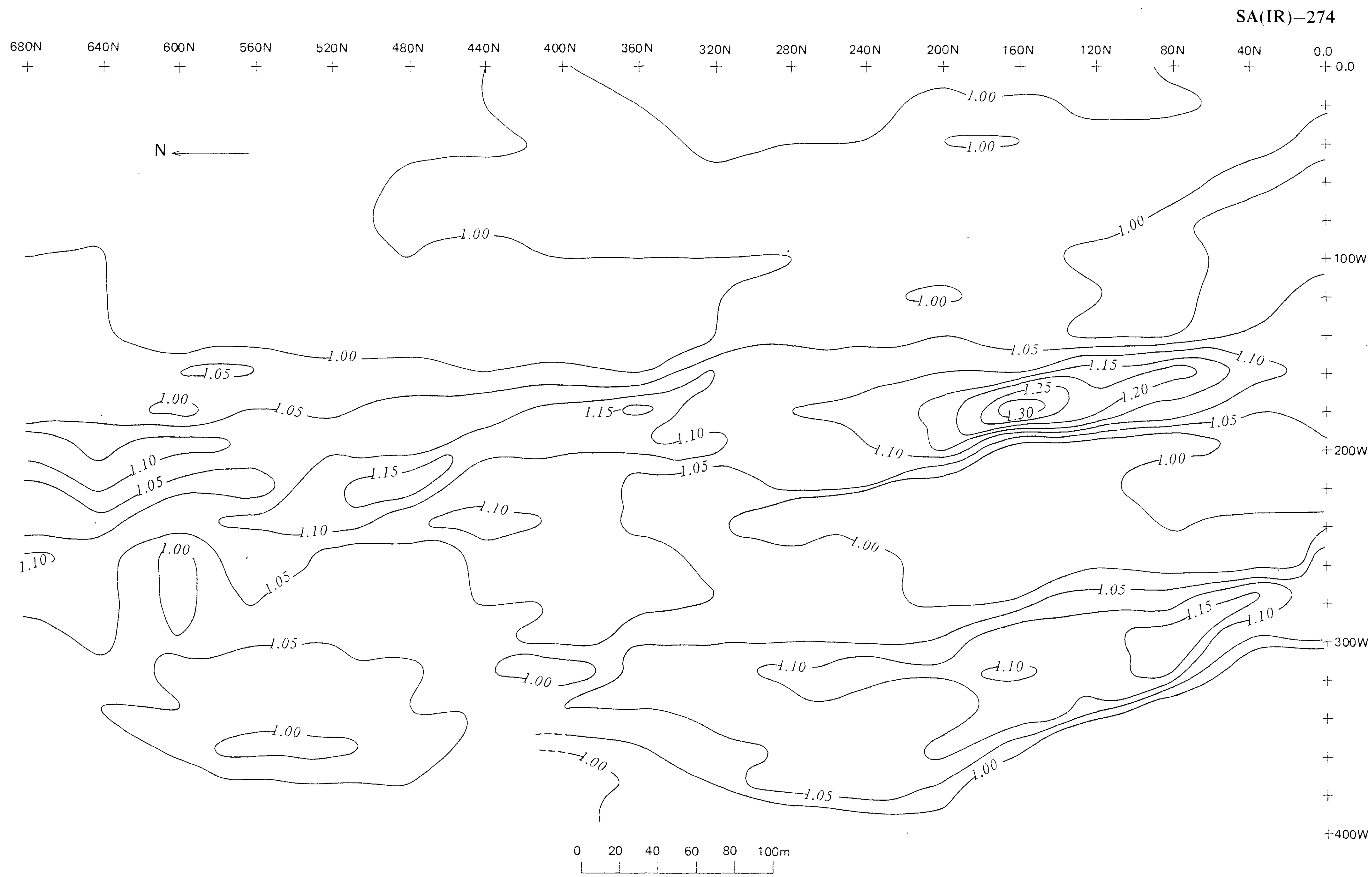

Figure 12.--Electromagnetic ratio map of Wadi Mandahah ancient mine. Contour interval 0.05.